surface normal ν. With regard to the orientation of the sample crystal in the experiment we chose the coordinate set as shown in Fig. 1. We can express the dispersion equation (1) explicitly:

$$C_3^a z^3 + C_2^a z^2 + C_1^a z + C_0^a = 0, \quad (1a)$$

$$C_3^a = -2\sin\gamma(3-4\sin^2\gamma),$$

$$C_2^a = 3[2\cos\gamma(1-4\sin^2\gamma)x - kB_0'],$$

$$C_1^a = 6\sin\gamma(3-4\sin^2\gamma)x^2,$$

$$C_0^a = 2\cos\gamma(1-4\sin^2\gamma)x^3 - 3kB_0'x^2 + k^3(B_0'^3 - 3B_0'B^2 + 2B^3);$$

$$C_6^b z^6 + C_4^b z^4 + C_3^b z^3 + C_2^b z^2 + C_1^b z + C_0^b = 0, \quad (1b)$$

$$C_6^b = -1,$$

$$C_4^b = -3[x^2 - k^2(1+B_0)],$$

$$C_3^b = -2\sin\gamma\, k_m^3(3-4\sin^2\gamma),$$

$$C_2^b = 3[-x^4 + 2k^2(1+B)x^2 + 2k_m^3\cos\gamma(1-4\sin^2\gamma)x + C^b],$$

$$C_1^b = 6k_m^3\sin\gamma(3-4\sin^2\gamma)x^2,$$

$$C_0^b = -x^6 + 3k^2(1+B_0)x^4 - 2k_m^3\cos\gamma(1-4\sin^2\gamma)x^3 + 3C^b x^2 + k^6[(1+B_0)^3 - 3(1+B_0)B^2 + 2B^3] - k_m^6 + 3k_m^2 C^b,$$

$$C^b = k^2\{k_m^2(1+B_0) - k^2[(1+B_0)^2 - B^2]\};$$

$$C_4^c z^4 + C_3^c z^3 + C_2^c z^2 + C_1^c z + C_0^c = 0, \quad (1c)$$

$$C_4^c = 3 - 4\sin^2\gamma,$$

$$C_3^c = 2\sin\gamma[4x\cos\gamma + kB_0' - k_m(3-4\sin^2\gamma)],$$

$$C_2^c = 2x^2 + 2\cos\gamma[3k_m(1-4\sin^2\gamma) - kB_0']x - [k^2(1+B_0) - k_m^2](3-4\sin^2\gamma) - 4kk_mB_0'\sin^2\gamma - k^2(B_0'^2 - B^2),$$

$$C_1^c = 2\sin\gamma(4\cos\gamma\, x^3 + [kB_0' + 3k_m(3-4\sin^2\gamma)]x^2 + 4\cos\gamma\{kk_mB_0' - [k^2(1+B_0) - k_m^2]\}x - C^c),$$

$$C_0^c = -(1-4\sin^2\gamma)x^4 - 2\cos\gamma[kB_0' + k_m(1-4\sin^2\gamma)]x^3 + \{[k^2(1+B_0) - k_m^2] \times (1-4\sin^2\gamma) - 4kk_mB_0'\cos^2\gamma - k^2(B_0'^2 - B^2)\}x^2 + 2\cos\gamma\, C^c x - k^2k_m^2(B_0'^2 - B^2) + k^4\{B^2[2B - (1+B_0)] + B_0'[B_0'(1+B_0) - 2B^2]\},$$

$$C^c = k\{k^2[B_0'(1+B_0) - B^2] - k_m^2B_0' - kk_m(B_0'^2 - B^2)\}.$$

The coordinate x is related to the angle of incidence of the incident wave by

$$x(\theta) = k_m\cos(60+\gamma) - k\cos(60+\gamma+\theta).$$

When the incident beam is not the extremely asymmetrical one, the function $x(\theta)$ can be expressed as the linear one

$$x(\theta) = -\delta k\cos(60+\gamma) + k\theta\sin(60+\gamma).$$

References

BEDYŃSKA, T. (1973). *Phys. Status Solidi A*, **19**, 365–372.

CHANG, S. L. (1984). *Springer Series in Solid-State Sciences*, Vol. 50, pp. 72–80. Berlin: Springer.

DESLATTES, R. D. (1968). *Appl. Phys. Lett.* **12**, 133–135.

DRAHOKOUPIL, J. & FINGERLAND, A. (1982). *Advances in X-ray Spectroscopy*, edited by C. BONNELLE & C. MANDÉ, pp. 167–201. Oxford: Pergamon Press.

GRAEFF, W. & BONSE, U. (1977). *Z. Phys.* **B27**, 19–32.

PACHEROVÁ, O. & BUBÁKOVÁ, R. (1987). *Acta Cryst.* **A43**, 161–167.

PENNING, P. & POLDER, D. (1968). *Philips Res. Rep.* **23**, 1–12.

Acta Cryst. (1994). **A50**, 224–231

Dynamical X-ray Diffraction from Imperfect Crystals: a Solution Based on the Fokker–Planck Equation

BY T. J. DAVIS

CSIRO Division of Materials Science and Technology, Private Bag 33, *Rosebank MDC, Clayton, Victoria* 3169, *Australia*

(*Received* 24 *May* 1993; *accepted* 7 *September* 1993)

Abstract

A stochastic model of crystal defects is incorporated into a Fokker–Planck equation describing dynamical X-ray diffraction from imperfect extended-face crystals. The Fokker–Planck equation is solved by forming a set of complex moments describing the reflectance fluctuations in the crystal. This leads to

an infinite set of coupled differential equations that are solved by neglecting high-order moments and numerically integrating the equations. The numerical solutions of X-ray rocking curves from a set of imperfect silicon films show excellent agreement with a Monte Carlo simulation and with a kinematical calculation away from the Bragg peak. The dynamical equations are suitable for describing Bragg diffraction from extended-face crystals containing defects, strain and composition variations.

Introduction

The dynamical theory of X-ray diffraction is required to properly describe the interplay between the incident and the diffracted wave fields in crystals. The Takagi–Taupin equations (Takagi, 1962, 1969; Taupin, 1964) usually provide the basis for calculations of diffraction from distorted crystals. These are a coupled set of differential equations for the complex wave amplitudes in the crystal and can be solved numerically to describe diffraction from crystals containing strain, compositional variations or even dislocations (Epelboin & Authier, 1983). However, the calculation of X-ray diffraction from crystals containing large numbers of defects is more difficult because of the random nature of the defects and the strain fields they produce. Instead, statistical theories have been developed (Zachariasen, 1967; Kato, 1980; Kulda, 1987, 1988; Becker & Al Haddad, 1990, 1992; see also the review in Schneider, Bouchard, Graf & Nagasawa, 1992) in which averages are taken over an ensemble of defects and which require the solution of equations for the diffracted intensities.

A completely different approach was taken by Davis (1991), by whom the problem of Bragg diffraction from an extended-face crystal containing randomly distributed defects was transformed into a Fokker–Planck equation for the probability density describing the complex reflectance. The effect of the defects on the phase of the X-ray beam was treated in a fashion similar to the treatment of molecular collisions in the statistical theory of Brownian motion (Uhlenbeck & Ornstein, 1930). This results in a stochastic differential equation, known as the Langevin equation, which is used to derive a correlation function for the strain fluctuations in the crystal. A stochastic defect model was later developed (Davis, 1992), in which considerations of the strain and strain-gradient fluctuations associated with stacking faults and misoriented crystal grains led naturally to the Langevin equation. It was shown that the phase correlation function of Becker & Al Haddad (1989, 1990) was a special case of the phase-correlation function derived from the Langevin equation. The correlation function compared favourably with that obtained from X-ray diffraction data using a kinematical theory (Davis, 1993).

In this paper, the Fokker–Planck equation is used to derive an infinite set of coupled differential equations describing dynamical diffraction from imperfect crystals. By being truncated at low orders, the equations are integrated numerically to solve for the reflectivity of the imperfect crystal. A Monte Carlo method for the solution of diffraction problems is also devised. The results of calculations using the dynamical equations, the Monte Carlo method and the kinematical theory are compared.

Theory

The variation of the reflectance $R(t)$ with depth t in a crystal can be derived from the Takagi–Taupin equations and takes the form of a complex Riccati equation,

$$dR/dt = i\alpha(\chi_h - 2\beta R + \chi_{-h}R^2), \qquad (1)$$

where $\alpha = -\pi k/\gamma_h$, $1/k = \lambda$ is the X-ray wavelength, γ_o and γ_h are the direction cosines of the transmitted and diffracted waves, with respect to the coordinate axis, $\chi_h = C\chi_h'$ and $\chi_{-h} = -C(\gamma_h/\gamma_o)\chi'^2_{-h}$ where C is a polarization factor and χ_h' is the complex Fourier component of the dielectric susceptibility associated with reciprocal-lattice vector $\mathbf{h}$. The resonance parameter, β, is given by

$$\beta = n^2[(k_h^2 - k^2)/2k^2] - n[\hat{\mathbf{k}}_h \cdot \nabla(\mathbf{h}\cdot\mathbf{v})/k], \qquad (2)$$

where $n = (1 + \chi_o')^{1/2}$ is the refractive index for the X-rays, $\mathbf{k}$ and $\mathbf{k}_h$ are the wave vectors of the transmitted and diffracted waves in the crystal interior, $\hat{\mathbf{k}}_h$ is the unit vector in the direction of $\mathbf{k}_h$ and $\mathbf{v}$ is the displacement of a point in the lattice from its relaxed position resulting from strains in the crystal.

The defects in the crystal disrupt the lattice and introduce strain fields that may extend throughout the entire crystal. In the following statistical description of defects, these strain fields are decomposed into a smoothly varing component, which is the average of all the strains over a plane at depth t, and a discontinuous random component. The contribution to the resonance parameter of all continuous strain fields in the crystal and the average strain field associated with the defects, together with the first term on the right side of (2), is denoted $\langle\beta\rangle$. The contribution from the random strain fluctuations arising from the defects is then written as $\beta_\xi(t) = \beta(t) - \langle\beta(t)\rangle$ so that $\langle\beta_\xi(t)\rangle = 0$. If the crystal contains defects that introduce discontinuities in the strain or the strain gradient (and hence in β_ξ and $d\beta_\xi/dt$) and that are Gaussian distributed with zero mean over the plane at depth t, then it can be shown (Davis, 1992) that the fluctuations in the resonance

parameter obey a Langevin equation,

$$l\,\mathrm{d}\beta_\xi(t)/\mathrm{d}t + \beta_\xi(t) = \sigma\xi(t), \tag{3}$$

where l is a *correlation length* and σ determines the *strength* of the defects. The correlation length represents a characteristic distance between strain fluctuations. $\xi(t)$ is a Gaussian-distributed random variable with zero mean and δ-function correlation,

$$\langle\xi(t)\xi(t+\tau)\rangle = \delta(\tau). \tag{4}$$

According to the central-limit theorem in the theory of statistics, sums of independent random variables tend to be Gaussian distributed (see *e.g.* Kendall & Stuart, 1969), so that, provided there are a large number of defects, the assumption of Gaussian-distributed variables $\xi(t)$ is not a major limitation. The solution to the Langevin equation (3) leads to a correlation function for β_ξ,

$$\langle\beta_\xi(t)\beta_\xi(t+\tau)\rangle = \nu^2\exp(-|\tau|/l), \tag{5}$$

where the variance of the distribution $\nu^2 = \sigma^2/2l$. The above set of equations may be considered to form the basis of the stochastic model of crystal defects.

A broad X-ray beam diffracting from an extended-face crystal is described by the average reflectivity, $\langle R^*R\rangle$. To form this average, an explicit solution for R is required. Since (1) is a Riccati equation, it is not possible to write down the general solution for R in terms of integrals involving $\beta(t)$, α, χ_h and χ_{-h} when $\beta(t)$ is an arbitrary function of t (Forsyth, 1943; Brand, 1966). It is this fact that makes it difficult to solve problems involving dynamical X-ray diffraction and that usually leads to rather complicated approximate solutions. Indeed, (1) is usually solved numerically (*e.g.* Bensoussan, Malgrange & Sauvage-Simkin, 1987). In the present stochastic model, $\beta(t)$ is not only a function of t but it is also an *unknown* function as it contains the random variable β_ξ for which only the statistical properties are known, through (3), (4) and (5). This difficulty was overcome by Davis (1991), who transformed the problem so that R and β_ξ were no longer treated as functions of t but were considered as coordinates in a three-dimensional space. If $R = x + iy$, then the reflectance of a crystal is determined by a density function in this space, $u(x, y, \beta_\xi; t)$, where t is treated as a parameter. For example, the mean reflectivity is given by

$$\langle R^*(t)R(t)\rangle = \iiint(x^2+y^2)u(x,y,\beta_\xi;t)\,\mathrm{d}x\,\mathrm{d}y\,\mathrm{d}\beta_\xi, \tag{6}$$

where the integration for x and y is over the unit circle and that for β_ξ is over $(-\infty, \infty)$. Because the density function is normalized to unity over all space, it can be thought of as the probability density for the crystal having reflectance $x + iy$ and a resonance parameter $\langle\beta\rangle + \beta_\xi$ at depth t.

If the equation for the reflectance variation (1) is written in terms of real and imaginary components,

$$\mathrm{d}R/\mathrm{d}t = V_x + iV_y \equiv V, \tag{7}$$

then, together with the stochastic defect model, it can be shown (Davis, 1991) that the probability density function obeys the Fokker–Planck equation,

$$\partial u/\partial t = -\partial(V_x u)/\partial x - \partial(V_y u)/\partial y + \partial(\beta_\xi u/l)/\partial\beta_\xi + (\sigma^2/2l^2)\partial^2 u/\partial\beta_\xi^2. \tag{8}$$

In general, Fokker–Planck equations are difficult to solve analytically. Instead, to demonstrate the validity of the equation, a numerical solution is sought based on a set of complex moments generated from (8). As shown below, the moments are described by an infinite set of coupled first-order differential equations in t. For many applications, the set of equations can be truncated at very low orders and still produce accurate results.

To proceed, several points concerning the density function u are required:

(1) For any function f of x, y and β_ξ, the average is given by

$$\langle f(x,y,\beta_\xi)\rangle = \iiint f(x,y,\beta_\xi)u(x,y,\beta_\xi)\,\mathrm{d}x\,\mathrm{d}y\,\mathrm{d}\beta_\xi, \tag{9}$$

where the integrals are over all space.

(2) If f represents any polynomial in x, y and β_ξ, then as x, y and β_ξ approach their limits (*i.e.* the unit circle for x and y, $\pm\infty$ for β_ξ) the product of f and u, or of f and any derivative of u, tends to zero.

(3) The average gradient of any function $f(x, y, \beta_\xi)$ is related to the gradient of u using an integration by parts,

$$\begin{aligned}\iiint f(x,y,\beta_\xi)\partial u/\partial x\,\mathrm{d}x\,\mathrm{d}y\,\mathrm{d}\beta_\xi &= \iiint[\partial(fu)/\partial x - u\partial f/\partial x]\,\mathrm{d}x\,\mathrm{d}y\,\mathrm{d}\beta_\xi \\ &= -\iiint u\partial f/\partial x\,\mathrm{d}x\,\mathrm{d}y\,\mathrm{d}\beta_\xi \\ &= -\langle\partial f/\partial x\rangle,\end{aligned} \tag{10}$$

where the first term in the integral is zero, by point (2) above. Similar equations apply for derivatives with respect to y and β_ξ. Furthermore, the average of f with respect to the second derivative of u leads to

$$\iiint f(x,y,\beta_\xi)\partial^2 u/\partial x^2\,\mathrm{d}x\,\mathrm{d}y\,\mathrm{d}\beta_\xi = \langle\partial^2 f/\partial x^2\rangle. \tag{11}$$

One of the requirements of the numerical solution is that it reduces to the perfect-crystal case when there are no defects. This is ensured by use of the fluctuations in the reflectance $\delta R(t) = R - \langle R(t)\rangle$, where $\langle R(t)\rangle$ is the mean reflectance and

$$\langle R^*R\rangle = \langle R^*\rangle\langle R\rangle + \langle\delta R^*\delta R\rangle. \tag{12}$$

The mean reflectance obeys the equation

$$\begin{aligned} \mathrm{d}\langle R\rangle/\mathrm{d}t &= i\alpha(\chi_h - 2\langle\beta\rangle\langle R\rangle + \chi_{-h}\langle R\rangle^2 - 2\langle\beta_\xi\delta R\rangle \\ &\quad + \chi_{-h}\langle\delta R^2\rangle) \\ &\equiv \langle V\rangle, \end{aligned} \tag{13}$$

which depends on averages of products of fluctuations, such as $\langle\beta_\xi\delta R\rangle$, which are called *complex moments*. In the absence of defects, the moments are zero and the perfect-crystal equation is returned. The problem is to find an equation for the variation of these moments with depth in the crystal. For this purpose, consider the most general moment, $\langle\delta R^{*a}\delta R^b\beta_\xi^c\rangle$ and its derivative with respect to t,

$$\begin{aligned} &\mathrm{d}\langle\delta R^{*a}\delta R^b\beta_\xi^c\rangle/\mathrm{d}t \\ &= \iiint\delta R^{*a}\delta R^b\beta_\xi^c\partial u/\partial t\,\mathrm{d}x\,\mathrm{d}y\,\mathrm{d}\beta_\xi \\ &\quad - \iiint(a\delta R^{*a-1}\delta R^b\beta_\xi^c u\,\mathrm{d}\langle R^*\rangle/\mathrm{d}t \\ &\quad + b\delta R^{*a}\delta R^{b-1}\beta_\xi^c u\,\mathrm{d}\langle R\rangle/\mathrm{d}t)\,\mathrm{d}x\,\mathrm{d}y\,\mathrm{d}\beta_\xi \\ &= \iiint\delta R^{*a}\delta R^b\beta_\xi^c\partial u/\partial t\,\mathrm{d}x\,\mathrm{d}y\,\mathrm{d}\beta_\xi \\ &\quad - a\langle\delta R^{*a-1}\delta R^b\beta_\xi^c\langle V^*\rangle\rangle \\ &\quad - b\langle\delta R^{*a}\delta R^{b-1}\beta_\xi^c\langle V\rangle\rangle, \end{aligned} \tag{14}$$

where the last two terms arise from the dependence of $\delta R(t)$ on $\langle R(t)\rangle$. The complex function $\langle V\rangle$ is defined by (13).

When the derivative of u with respect to t in (14) is replaced by the Fokker–Planck equation (8), integrals of 'spatial' derivatives of u arise. Consider the term involving $\partial(V_x u)/\partial x$ and apply (10), then

$$\begin{aligned} &\iiint\delta R^{*a}\delta R^b\beta_\xi^c\partial(V_x u)/\partial x\,\mathrm{d}x\,\mathrm{d}y\,\mathrm{d}\beta_\xi \\ &\quad = -a\langle\delta R^{*a-1}\delta R^b\beta_\xi^c V_x\partial R^*/\partial x\rangle \\ &\quad\quad - b\langle\delta R^{*a}\delta R^{b-1}\beta_\xi^c V_x\partial R/\partial x\rangle. \end{aligned} \tag{15}$$

Similar expressions are obtained for $\partial(V_y u)/\partial y$ and $\partial(\beta_\xi u/l)/\partial\beta_\xi$. Note that $\partial R/\partial x = \partial R^*/\partial x = 1$ and $\partial R/\partial y = -\partial R^*/\partial y = i$. The occurrence of the imaginary term with V_y allows the result to be written in terms of the complex function $V = V_x + iV_y$. If (11) is used for the term involving $\partial^2 u/\partial\beta_\xi^2$, then (14) becomes

$$\begin{aligned} &\mathrm{d}\langle\delta R^{*a}\delta R^b\beta_\xi^c\rangle/\mathrm{d}t \\ &\quad = a\langle\delta R^{*a-1}\delta R^b\beta_\xi^c(V^* - \langle V^*\rangle)\rangle \\ &\quad\quad + b\langle\delta R^{*a}\delta R^{b-1}\beta_\xi^c(V - \langle V\rangle)\rangle \\ &\quad\quad - (c/l)\langle\delta R^{*a}\delta R^b\beta_\xi^c\rangle \\ &\quad\quad + (\sigma^2/2l^2)c(c-1)\langle\delta R^{*a}\delta R^b\beta_\xi^{c-2}\rangle. \end{aligned} \tag{16}$$

The term $V - \langle V\rangle$ can be obtained from the difference between (1) and (13),

$$\begin{aligned} V - \langle V\rangle &= i\alpha[\chi_{-h}(\delta R^2 - \langle\delta R^2\rangle + 2\langle R\rangle\delta R) - 2(\beta_\xi\delta R \\ &\quad - \langle\beta_\xi\delta R\rangle + \beta_\xi\langle R\rangle + \langle\beta\rangle\delta R)]. \end{aligned} \tag{17}$$

This is substituted into (16) and the various terms are expanded in a straightforward manner. Since the complex moments represent the diffuse scattering terms, let the matrix element $D_{abc} = \langle\delta R^{*a}\delta R^b\beta_\xi^c\rangle$; then, the set of equations describing dynamical diffraction in an imperfect crystal is

$$\begin{aligned} \mathrm{d}D_{abc}/\mathrm{d}t &= i\alpha(bJ_{abc} - aJ^*_{bac}) - (c/l)D_{abc} \\ &\quad + (\sigma^2/2l^2)c(c-1)D_{ab(c-2)}, \end{aligned} \tag{18}$$

$$\begin{aligned} J_{abc} &= \chi_{-h}(2\langle R\rangle D_{abc} + D_{a(b+1)c} \\ &\quad - D_{020}D_{a(b-1)c}) - 2\langle\beta\rangle D_{abc} - 2\langle R\rangle D_{a(b-1)(c+1)} \\ &\quad - 2D_{ab(c+1)} + 2D_{011}D_{a(b-1)c}, \end{aligned} \tag{19}$$

$$\begin{aligned} \mathrm{d}\langle R\rangle/\mathrm{d}t &= i\alpha(\chi_h - 2\langle\beta\rangle\langle R\rangle + \chi_{-h}\langle R\rangle^2 - 2D_{011} \\ &\quad + \chi_{-h}D_{020}), \end{aligned} \tag{20}$$

$$\langle R^*R\rangle = \langle R^*\rangle\langle R\rangle + D_{110}. \tag{21}$$

The matrix element J_{abc} has been introduced for convenience. Since the mean fluctuations $\langle\delta R^*\rangle = \langle\delta R\rangle = 0$, then $D_{100} = D_{010} = 0$, always. Furthermore, it is easily shown that $D_{000} = 1$ and $D_{abc} = D^*_{bac}$.

Equations (18) represent an infinite set of coupled differential equations. For many applications, only the lower-order terms in a, b and c are significant and, given a set of initial conditions, the equations can be integrated numerically. These initial conditions depend on the problem being solved. As an example, consider the Bragg diffraction from the upper face of a thin film and take the lower face as the coordinate origin. In this example, the equations (18) are integrated numerically from the lower face to the upper face, where the diffracted X-ray beam emerges. Initial conditions are therefore required at the lower face. Since there is no diffracted beam there, the reflectance and the reflectance fluctuations are zero, so that $\langle R(t=0)\rangle = 0$ and $D_{abc}(t=0) = 0$, provided $a \neq 0$ and $b \neq 0$. At the lower face of the film, there are defects that are assumed to be Gaussian distributed. If the distribution is stationary, *i.e.* does not depend on t, then the terms D_{00c} represent the moments of the Gaussian distribution. In this case, $D_{00(2n-1)} = 0$ and $D_{002n} = \nu^{2n}(2n)!/(2^n n!)$, where n is an integer and $\nu^2 = \sigma^2/2l$ is the variance. The fact that this leads to a stationary distribution with t can be verified by substitution into (18).

As a means of testing the dynamical equations (18)–(21), a numerical simulation of X-ray diffraction from an imperfect crystal was performed using a computer to randomly generate values of β_ξ and to calculate the dynamical reflectance. The basis of this *Monte Carlo* simulation is discussed below. Then, comparisons between the simulation, the dynamical equations and a kinematical solution are made.

Monte Carlo simulation

To simulate the dynamical diffraction, the imperfect crystal is divided into a large stack of perfect-crystal slabs. Each slab has a thickness t_s. Since these are perfect, an explicit solution of (1) can be used,

$$R(t) = R_o + [R(t') - R_o]\exp[2i\alpha\omega(t - t')] \times (1 + [R(t') - R_o](\chi_{-h}/2\omega) \times \{1 - \exp[2i\alpha\omega(t - t')]\})^{1/2}, \quad (22)$$

$$\omega = \pm(\beta^2 - \chi_{-h}\chi_{-h})^{1/2} \quad (23)$$

$$R_o = (\beta + \omega)/\chi_{-h}, \quad (24)$$

where $R(t')$ is the reflectance at t', $R_o(\beta)$ is the reflectance of the thick perfect crystal with resonance parameter β and the sign of the parameter ω is chosen so that $|R_o| < 1$.

The aim is to randomly select from a Gaussian distribution a value of β_ξ for the lower face of the crystal where $R(0) = 0$, calculate the appriate values $\beta = \langle\beta\rangle + \beta_\xi$, ω and R_o and then use (22) to calculate $R(t_s)$ at the upper surface of the first slab. Then another value of β_ξ is selected and the reflectance at the top of the next slab is calculated, using $R(t_s)$ as an initial condition. This is repeated until the reflectance at the upper surface of the imperfect crystal is obtained. This represents one point of a statistical ensemble. The entire procedure is repeated many times and the average reflectivity $\langle R^*R\rangle$ is calculated.

Although the value of β_ξ at the lower face is randomly selected from a Gaussian distribution, all subsequent values depend on the previous values in accordance with the correlation length l in the crystal. For example, if the correlation length is large compared with t_s, then subsequent values of β_ξ will not differ much from the first value, *i.e.* they are correlated in some way. The correct probability distribution for β_ξ can be obtained from the Fokker–Planck equation (8) by neglecting the reflectance terms, yielding

$$\partial u/\partial t = \partial(\beta_\xi u/l)/\partial\beta_\xi + (\sigma^2/2l^2)\partial^2 u/\partial\beta_\xi^2. \quad (25)$$

This represents the Ornstein–Uhlenbeck process (Uhlenbeck & Ornstein, 1930), which, given a value $\beta_{\xi o}$ at t_o, has a solution for β_ξ at t (Risken, 1984):

$$u(\beta_\xi, t|\beta_{\xi o}, t_o) = (\pi(\sigma^2/l)\{1 - \exp[-2(t - t_o)/l]\})^{-1/2} \times \exp[-\{\beta_\xi - \beta_{\xi o}\exp[-(t - t_o)/l]\}^2 \times ((\sigma^2/l)\{1 - \exp[-2(t - t_o)/l]\})^{-1}]. \quad (26)$$

When $t - t_o >> l$, β_ξ becomes independent of $\beta_{\xi o}$ and is Gaussian distributed. When $t - t_o << l$, the distribution becomes sharply peaked about $\beta_{\xi o}$. The distribution (26) is used in conjunction with a pseudorandom number generator to determine the value of β_ξ in each slab, given its value in the previous slab. Provided t_s is not much larger than l and 50 slabs or more are used to represent the crystal, then consistent results are obtained from the Monte Carlo program.

Numerical tests of the theory

The dynamical equations for the imperfect crystal were solved numerically to produce rocking curves for a set of silicon films of various thicknesses containing defects characterized by different correlation lengths and defect strengths. The same defect parameters were used in the Monte Carlo program to provide data to compare with the results obtained from the dynamical equations. In addition, the kinematical diffraction was also calculated using the procedure described by Davis (1992). This last comparison is quite important because the kinematical method has already been used to compare the stochastic model with X-ray data from thin films (Davis, 1993). Although it is based on the same stochastic equations, the kinematical method involves calculations that are quite different from those required in the dynamical method. The kinematical rocking curves should agree with the dynamical curves at angles well away from the Bragg angle, where dynamical effects are less important.

The integrations of (18) and (20) were performed using an adaptive step-size fifth-order Runge–Kutta method employing complex arithmetic. This is a modification of the routine described by Press, Flannery, Teukolsky & Vetterling (1987), which monitors the integration errors in $\langle R\rangle$, D_{011}, D_{020} and D_{110} and adjusts the integration step to ensure a predetermined level of accuracy. The three film thicknesses used in the calculation were chosen to cover a range of values about the dynamical extinction length for the silicon 111 reflection, which is about 0.75 μm for X-rays of wavelength 1.54 Å. Because highly imperfect crystals behave kinematically, the defect strengths were kept small to maintain dynamical characteristics. Correlation lengths were chosen to represent the range from almost point-like defects (l = 0.01 μm) to mosaic blocks (l = 1 μm). Ideally, the correlation length for point defects is $l = 0$; however, the third term on the right of (18) depends on $1/l$, which diverges as l approaches zero. This term also makes the integrations of (18) very slow because the step interval cannot be much larger than l, otherwise the integration errors become large.

The data for each calculation are given in Table 1. The columns labelled max. a, max. b and max. c refer to the maximum index used in D_{abc}. All moments with indices exceeding the maxima were set to zero. The number of trials refers to the number of reflectivities used in the Monte Carlo program to

Table 1. *Summary of conditions used in the simulations (see text for details)*

Film and defect data				Dynamical equations			Monte Carlo	
Figure	Thickness (μm)	l(μm)	ν^2	Max.a	Max.b	Max.c	No. of trials	t_s(μm)
1	0.5	0.01	1×10^{-9}	2	2	2	100	0.005
1	2	0.01	1×10^{-9}	2	2	2	100	0.02
1	10	0.01	1×10^{-9}	3	3	3	50	0.01
2	0.5	0.1	5×10^{-10}	2	2	2	100	0.005
2	2	0.1	5×10^{-10}	2	2	2	100	0.02
2	10	0.1	5×10^{-10}	3	3	3	100	0.02
3	0.5	1.0	5×10^{-11}	3	3	6	100	0.005
3	2	1.0	5×10^{-11}	3	3	6	100	0.05
3	10	1.0	5×10^{-11}	3	3	9	100	0.05

calculate the average at each rocking angle. The last column gives the slab thickness, t_s. The results of the calculations are shown in Figs. 1, 2 and 3. In most cases, the results from the dynamical equations (solid lines) show excellent agreement with the Monte Carlo program (points), and also with the kinematical results (dashed lines) away from the Bragg peaks. Near the Bragg peaks, the kinematical reflectivities diverge, as expected. The divergences of the kinematical results at large angles are artifacts of the convolution process used in the calculations.

Discussion

The main limitation of this dynamical method is the number of coupled equations required to obtain accurate results when the crystals are thick and the defect strengths or the correlation lengths are large. This limitation results from the use of moments to characterize the statistical nature of the diffraction. The high-order moments in β_ξ characterize the density $u(x, y, \beta_\xi; t)$ at large values of β_ξ. These represent regions of the crystal with large misorientations or large strain variations. Thus, large perturbations in the reflectance introduced by strong defects will require many high-order moments to represent accurately the density and to reproduce accurately the rocking curve. Furthermore, the magnitude of the perfect-crystal reflectance oscillates with t at a frequency $2\alpha\omega$ (the *Pendellösung* effect) and increases as the angle of incidence deviates further from the Bragg angle [see (22) and (23)]. Likewise, high-order moments in β_ξ oscillate rapidly and require small integration steps to minimize the integration errors. This slows the computations dramatically for incidence angles away from the Bragg angle. Thus, although the dynamical solution

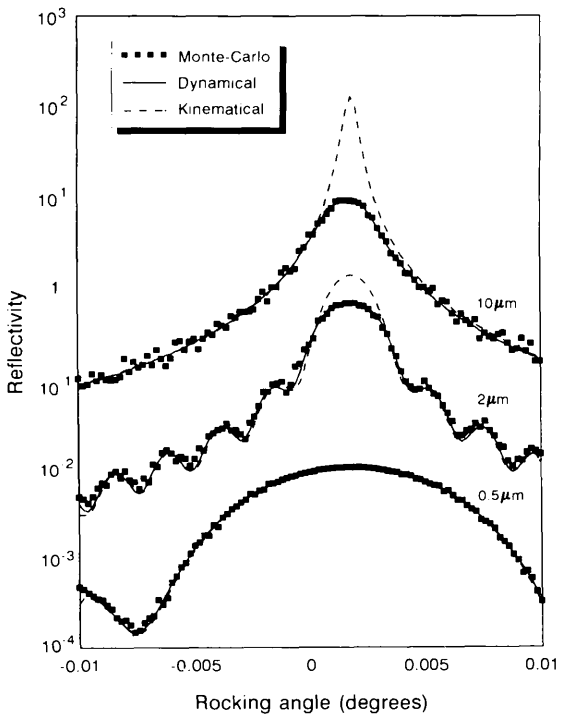

Fig. 1. Comparisons between the results of the dynamical, kinematical and Monte Carlo methods for imperfect silicon (111) films of various thicknesses for defect parameters $l = 0.01$ μm, $\nu^2 = 1\times10^{-9}$. The rocking curves for the 0.5 and the 10 μm films have been scaled by 0.1 and 10, respectively, to separate them for improved clarity. The X-ray wavelength was 1.54 Å. See Table 1 for additional information.

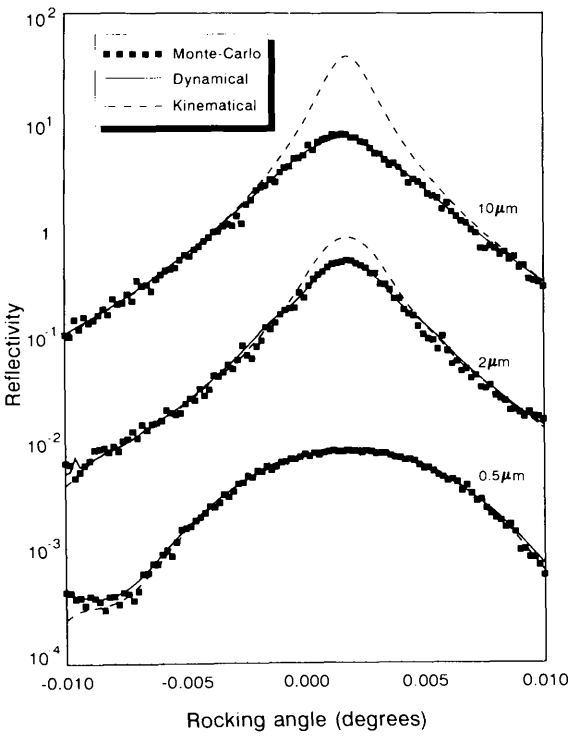

Fig. 2. Comparisons between the results of the dynamical, kinematical and Monte Carlo methods for imperfect silicon (111) films of various thicknesses for defect parameters $l = 0.1$ μm, $\nu^2 = 5\times10^{-10}$. The rocking curves for the 0.5 and the 10 μm films have been scaled by 0.1 and 10, respectively, to separate them for improved clarity. The X-ray wavelength was 1.54 Å. See Table 1 for additional information.

given in terms of moments is straightforward, it is not necessarily the most efficient or the most appropriate for computation. For example, an expansion using cumulants, or other functions that better characterize the distributions, might lead to fewer coupled equations and more accurate solutions. However, the solution in moments has demonstrated that the use of a density function obeying the Fokker–Planck equation yields results consistent with the Monte Carlo simulations and the kinematical theory for extended-face crystals. This theory is limited only by the applicability of the stochastic defect model.

The infinite set of equations (18) was terminated by setting all high-order moments to zero, leaving a small finite set to be integrated. Although this simple method worked well in the specific examples given, any finite number of moments generally constitutes a poor representation of a distribution (Van Kampen, 1976). Again, this relates to the previous point concerning the number of coupled equations required for accurate results. A better method is to introduce a closure rule, which is an approximation that allows the higher-order moments to be expressed in terms of the lower-order moments such that the equations can be written in a finite number of terms. The difficulty is in finding an approximation that does not compromise the accuracy of the solution. This requires specific knowledge of the problem being solved.

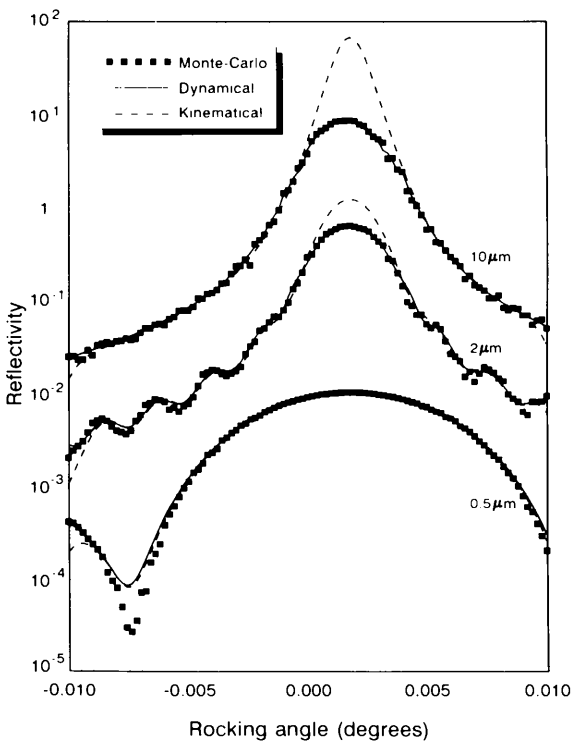

Fig. 3. Comparisons between the results of the dynamical, kinematical and Monte Carlo methods for imperfect silicon (111) films of various thicknesses for defect parameters $l = 1.0\ \mu m$, $\nu^2 = 5 \times 10^{-11}$. The rocking curves for the 0.5 and the 10 μm films have been scaled by 0.1 and 10, respectively, to separate them for improved clarity. The X-ray wavelength was 1.54 Å. See Table 1 for additional information.

As discussed above, the computation time increases as the angle of incidence shifts away from the Bragg angle. As an example, the calculation time per point for the 10 μm film in Fig. 3 was 430 s at $\theta - \theta_B = 0.01°$ but was 54 s at the Bragg angle (using a PC486 desk-top computer and allowing 1% integration errors). This should be compared with the kinematical calculation, which takes less than 1 s to compute the entire rocking curve. A more practical approach to X-ray diffraction from imperfect crystals is to use the kinematical method to calculate the rocking curve and to supplement this with dynamical equations where the kinematical results diverge about the Bragg peak.

Although the dynamical equations have only been demonstrated for homogeneous imperfect films, they are applicable to films that contain both compositional and strain variations, *i.e.* when $\chi_h(t)$, $\chi_{-h}(t)$ and $\langle\beta(t)\rangle$ are functions of t. For example, the equations may be used to model the diffraction of X-rays from imperfect strained-layer superlattices or for investigating diffraction from surface-damaged ion-implanted semiconductors.

Summary

A stochastic model of crystal defects has been incorporated into a theory for dynamical X-ray diffraction using a Fokker–Planck equation. The defects are assumed to cause Gaussian-distributed and independent fluctuations in the strain and strain gradients in the crystal. This gives rise to a Langevin equation, which, together with an equation for the crystal reflectance, leads to a Fokker–Planck equation for a density function describing the probability of finding a particular reflectance in the crystal. The Fokker–Planck equation is solved by the formation of a set of complex moments describing the reflectance fluctuations. This yields an infinite set of coupled differential equations for the reflectance in the imperfect crystal. The equations are solved by neglecting high-order moments and numerically integrating the equations. The results for X-ray diffraction from a set of silicon films showed excellent agreement with a Monte Carlo simulation and a kinematical calculation.

While the solution in moments has demonstrated that the Fokker–Planck equation is consistent with the Monte Carlo simulation and the kinematical theory, further work is required to find solutions that enable fast computation. The dynamical equations based on moments are suitable for describing diffrac-

tion from extended-face crystals containing defects, strain and compositional variations. The most practical application of the equations is to supplement the results of kinematical calculations near the Bragg angle.

References

BECKER, P. J. & AL HADDAD, M. (1989). *Acta Cryst.* A**45**, 333–337.

BECKER, P. J. & AL HADDAD, M. (1990). *Acta Cryst.* A**46**, 123–129.

BECKER, P. J. & AL HADDAD, M. (1992). *Acta Cryst.* A**48**, 121–134.

BENSOUSSAN, S., MALGRANGE, C. & SAUVAGE-SIMKIN, M. (1987). *J. Appl. Cryst.* **20**, 222–229.

BRAND, L. (1966). *Differential and Difference Equations*. New York: Wiley.

DAVIS, T. J. (1991). *Aust. J. Phys.* **44**, 693–704.

DAVIS, T. J. (1992). *Acta Cryst.* A**48**, 872–879.

DAVIS, T. J. (1993). *Acta Cryst.* A**49**, 755–762.

EPELBOIN, Y. & AUTHIER, A. (1983). *Acta Cryst.* A**39**, 767–772.

FORSYTH, A. R. (1943). *A Treatise on Differential Equations*, 6th ed. London: MacMillan.

KATO, N. (1980). *Acta Cryst.* A**36**, 763–769, 770–778.

KENDALL, M. G. & STUART, A. (1969). *The Advanced Theory of Statistics*, Vol. 1, 3rd ed. London: Griffin.

KULDA, J. (1987). *Acta Cryst.* A**43**, 167–173.

KULDA, J. (1988). *Acta Cryst.* A**44**, 283–285, 286–290.

PRESS, W. H., FLANNERY, B. P., TEUKOLSKY, S. A. & VETTERLING, W. T. (1987). *Numerical Recipes: the Art of Scientific Computing*. Cambridge Univ. Press.

RISKEN, H. (1984). *The Fokker–Planck Equation: Methods of Solution and Applications*. Berlin: Springer.

SCHNEIDER, J. R., BOUCHARD, R., GRAF, H. A. & NAGASAWA, H. (1992). *Acta Cryst.* A**48**, 804–819.

TAKAGI, S. (1962). *Acta Cryst.* **15**, 1311–1312.

TAKAGI, S. (1969). *J. Phys. Soc. Jpn*, **26**, 1239–1253.

TAUPIN, D. (1964). *Bull. Soc. Fr. Minéral. Cristallogr.* **87**, 469–511.

UHLENBECK, G. E. & ORNSTEIN, L. S. (1930). *Phys. Rev.* **36**, 823–841.

VAN KAMPEN, N. G. (1976). *Phys. Rep.* **24**, No. 3, 171–228.

ZACHARIASEN, W. H. (1967). *Acta Cryst.* **23**, 558–564.

Acta Cryst. (1994). A**50**, 231–238

Long-Period Modulated Structures of $Bi_2Sr_2(Ca_{1-x}Pr_x)Cu_2O_{8+\delta}$ Ceramics Studied by Electron Diffraction and High-Resolution Electron Microscopy

BY T. ONOZUKA

Institute for Materials Research, Tohoku University, Sendai 980, *Japan*

AND Y. HIROTSU

Nagaoka University of Technology, 1603-1 *Kamitomioka, Nagaoka* 940-21, *Japan*

(*Received* 17 *March* 1993; *accepted* 9 *August* 1993)

Abstract

Seven specimens of $Bi_2Sr_2(Ca_{1-x}Pr_x)Cu_2O_{8+\delta}$ ceramics in the concentration range $0 < x < 0.64$ have been prepared by solid-state reaction. The sample with $x = 0.16$ was examined in detail by means of electron diffraction and an intensity distribution of lattice reflections in reciprocal space was constructed on the basis of the experimental results. The intensity distribution is consistent with a calculation using a long-period modulated-structure (LPMS) model. This model with $b = 37b_0$ takes the $(3,1)_5$ mode of lattice modulation having the modulation period $2.31b_0$ (1.25 nm). The period is defined as the reciprocal of the wave number of a satellite reflection. The specimens with other concentrations also showed an intensity distribution of lattice reflections similar to that of $x = 0.16$. On the basis of the above results, lattice modulation periods have been examined for all the prepared specimens. The period decreases roughly from $\sim 1.2_8$ to $\sim 1.1_5$ nm with increasing concentration x. Seven modulation modes of the lattice have been determined by high-resolution observation; the modulation period of the LPMS model with each modulation mode is also nearly equal to the measured period.

1. Introduction

The superconducting ceramic $Bi_2Sr_2CaCu_2O_{8+\delta}$ has large lattice modulations along the b and c axes. Its basic structure is of the $Bi_4Ti_3O_{12}$ type with repeat b_0 (Fig. 1), having an orthorhombic lattice of unit-cell dimensions $a = a_0$, $b = b_0$ and $c = c_0$ ($a_0 \simeq b_0 \simeq 0.54$ and $c_0 \simeq 3$ nm). The lattice constants are taken as $a_0 = 2^{1/2}a_t$, $b_0 = 2^{1/2}a_t$ and $c_0 = 2c_t$, where a_t and c_t represent the values of the $Bi_4Ti_3O_{12}$-type structure.

The modulated structure has been intensively investigated by electron diffraction and high-resolution electron microscopy by Shaw, Shivashankar, La Placa, Cuomo, McGuire, Roy, Kelleher &